Available online at www.sciencedirect.com
ScienceDirect
Earth and Planetary Science Letters 257 (2007) 463–473
EPSL
www.elsevier.com/locate/epsl

Antarctic link to deep flow speed variation during Marine Isotope Stage 3 in the western North Atlantic

B.A.A. Hoogakker *, I.N. McCave, M.J. Vautravers [1]

Godwin Laboratory for Palaeoclimate Research, Department of Earth Sciences, University of Cambridge, Downing Street, Cambridge, CB2 3EQ, UK

Received 15 September 2006; received in revised form 15 February 2007; accepted 1 March 2007
Available online 12 March 2007
Editor: M.L. Delaney

Abstract

The Western Boundary Undercurrent (WBUC), off eastern America, is an important component of the Atlantic Meridional Overturning circulation and is the principal route for southward transport of North Atlantic waters and southward return of Southern Source Water (SSW). Here a direct flow speed proxy (mean grain size of the sortable silt) is used to infer the vigour of flow of the palaeo-WBUC at Blake Outer Ridge, (ODP Site 1060, depth 3481 m) during Marine Isotope Stage (MIS) 3. The overall shape of the flow speed proxy record shows a complex pattern of variability, with generally more vigorous flow and larger-scale flow variations between 35 and 60 ka than in the younger part of MIS 3 and MIS 2 (<35 ka). Six events of reduced bottom flow vigour (Slow Events, SEs) occur. These appear uncorrelated with Heinrich events, but are instead synchronous with the warming phases of Antarctic Warm Events A-1 to A-4 (with one new one, A-1a and one poorly defined, 'A-0'). This indicates that Antarctic climate exerts a stronger control on deep flow vigour in the North Atlantic during MIS 3 than Northern Hemisphere climate. The correspondence of SEs with Antarctic warming suggests a weaker WBUC flow due to reduced volume flux at SSW source or reduced SSW density. Because the variability of the lower limb of the WBUC was not connected to sharp North Atlantic changes in temperature, it is unlikely that the Dansgaard/Oeschger cycles were associated with a mode of MOC variation involving whole-ocean overturn, but more likely with perturbations of only the shallow Glacial Gulf Stream–Glacial Northern Source Intermediate Water cell. Nutrient proxies (benthic carbon isotopes and Cd/Ca of *Uvigerina peregrina*) at this site show similar trends to the GRIP $\delta^{18}O$ record. This correlation has previously been attributed mainly to hydrographic and flow changes but is here shown to be better explained by variations in surface ocean productivity and subsequent decomposition of ^{12}C rich organic material on the sea floor.

Keywords: Blake Outer Ridge; flow speed proxy; Western Boundary Undercurrent; Marine Isotope Stage 3; Slow Events; Northern and Southern Source Waters; warming phases of Antarctic Warm Event; density; geostrophic flow; Ocean Drilling Program; Joides Resolution; Leg 172; Site 1060, 1059

1. Introduction

The dynamic behaviour of systems may be more clearly revealed by examining their response to a series of rapid changes than by examining their behaviour at

* Corresponding author.
E-mail address: bhoo03@esc.cam.ac.uk (B.A.A. Hoogakker).
[1] Now at British Antarctic Survey, Madingley Road, Cambridge, CB3 0ET, UK.

0012-821X/$ - see front matter © 2007 Elsevier B.V. All rights reserved.
doi:10.1016/j.epsl.2007.03.003

two extreme steady states. For the ocean-climate system the two steady states may be represented by the last (and earlier) glacial maximum, and the Holocene. The response of the ocean to rapid changes is likely to be revealed by study of the period 60–30 ka in Marine Isotope Stage (MIS) 3, particularly in the North Atlantic. In the Northern Hemisphere MIS 3 is characterized by a series of abrupt climatic deteriorations with a pacing of 1500 to 4500 yr [1,2], possibly in multiples of ~1500 yr [3]. During Dansgaard/Oeschger (D/O) stadial (cold) intervals northern hemisphere climate was significantly cooler (5 to 10 °C), and dryer [4–8]. In North Atlantic marine sediment cores 'Heinrich layers' of large amounts of ice rafted debris (IRD) resulting from Northern Hemisphere ice sheet collapse, correlate with four severe D/O stadials in MIS 3 [9–11]. It has been suggested that these large climate oscillations were associated with perturbations in the ocean circulation, involving shifts in the location of deep water formation (from the Nordic Seas to areas south of Iceland) during 'normal' D/O stadials and cessation of all North Atlantic deep water formation during Heinrich events [3,12]. However, to date little direct evidence has been presented to support the suggestion that there may have been associated perturbations in the vigour of deep sea circulation. This is mainly because most chemical proxies used (including neodymium, Cd/Ca ratios and carbon isotopes ($\delta^{13}C$)) are indicators of the presence of a certain water mass or water mass nutrient content from which inference of circulation vigour may not be made [13], although they may reveal changes in water mass distributions.

Johnson et al. [14] were the first to study variations in the vigour of flow of the Western Boundary Undercurrent (WBUC) at Blake Outer Ridge (BOR) (Fig. 1), using sediment grainsize at two locations from ~3000 and 4000 m water depth. Their study provided low resolution data on grain size history for three main periods in the last 90 ka. Period I (90–30 ka) contains relatively coarse but variable mean grain sizes, hinting at strong and variable current speeds. During Period II (30–12 ka [^{14}C years]), which includes the Last Glacial Maximum (LGM), a steady decrease in mean grain size took place implying reduction to minimum flow speeds. Finally, Period III (12 ka–present) records an abrupt increase in mean grain size values with maximum values at ~9 ka [^{14}C years] suggesting rejuvenation of the WBUC.

Since then several other hypotheses have emerged challenging these views. For example Yu et al. [15], using radiochemical data, propose that the flux of

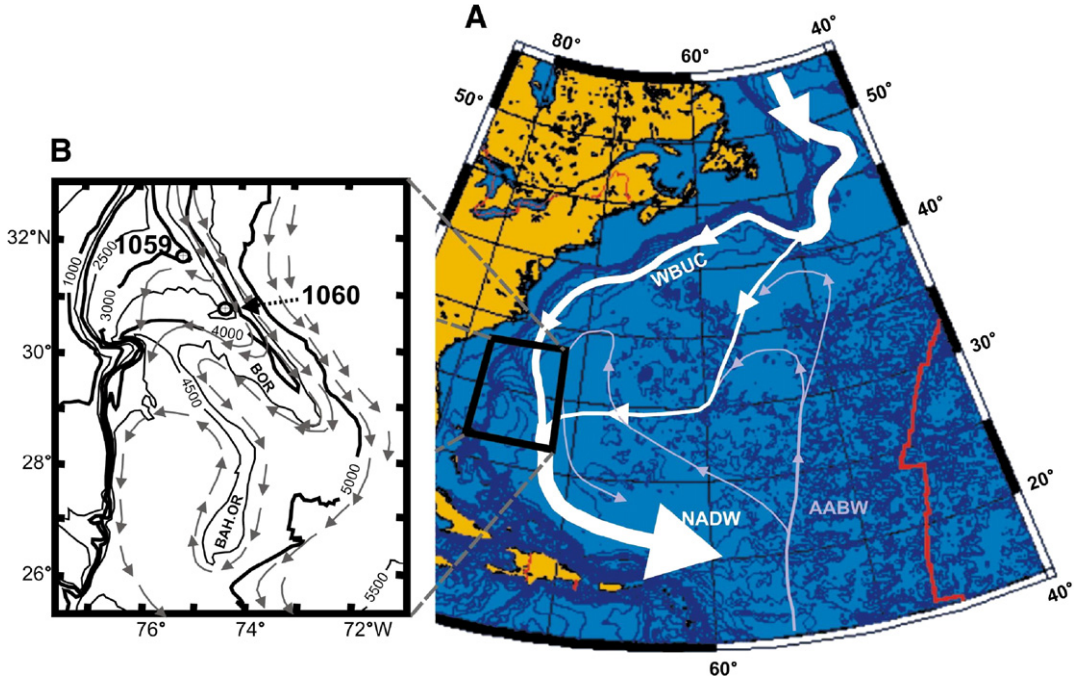

Fig. 1. A — Core location in the western North Atlantic. Deep flow directions are indicated, with WBUC (Western Boundary Undercurrent), NADW (North Atlantic Deep Water) and AABW (Antarctic Bottom Water, i.e. water containing evidence of a southern source). B — Detailed pattern of bottom currents around Blake Outer Ridge (BOR) and Bahama Outer Ridge (BAH.OR) (after McCave and Tucholke [68]).

Glacial Northern Source Intermediate Water (GNSIW[2]), essentially glacial Labrador/Irminger Sea/South Iceland Basin Water, was actually greater during the LGM even though the flux of Glacial Northern Source Deep Water (GNSDW, from the Nordic seas) was reduced or zero. This implies a stronger but shallower WBUC as this is the principal equatorward deep flow in the North Atlantic [16]. A stronger but shallower WBUC during glacials has also been inferred from grain size studies [17–21]. LGM reconstructions of $\delta^{13}C$ distributions also suggests suppression of GNSDW, with GNSIW <2500 m, whilst Southern Source Deep Water (GSSDW) occupied deeper areas [12,22].

The centre of the high velocity core of the WBUC presently flows around 3500 m near the upstream origin of BOR and deepens to ~4100 m downstream on its eastern flank at speeds of 20–22 cm s^{-1} [23]. In addition there may be a secondary axis of strong flow around 3600 water depth where speeds of 22 cm s^{-1} were measured by Jenkins and Rhines [24].

Here we present a high-resolution (average sample interval 100 yr) bottom flow vigour record for ODP Site 1060 (Blake Outer Ridge, 3481 m water depth) during MIS 3, using the mean grain size of the sortable silt size range (10–63 μm) as a physical flow speed proxy [25,26].

2. Location and material

Blake Outer Ridge (BOR) is situated in the westernmost part of the North Atlantic Ocean and lies adjacent to two important components of the Atlantic Meridional overturning circulation: the Gulf Stream and the WBUC, indeed the origin of the ridge has been ascribed to the cross-over of the two flows [27]. This location is very important for the latitudinal exchange of heat, salt and water.

The BOR is built by the rapid deposition of current-transported sediment and experiences strong bottom currents (Fig. 1). Because the BOR crest is isolated from the continental slope by a bathymetric low, occurrence of debris-flows and turbidites is precluded. BOR is a high accumulation sediment drift site (average accumulation rate ~45 cm ka^{-1}) and the core used here (ODP Site 1060, 30° 46′ N, 74° 28′ W, 3481 m water depth) provides an excellent record of climate variability at millennial to centennial time scales. At present the site is occupied by Northern Source Water components: Lower North Atlantic Deep Water (LNADW) supplied from the high latitude Norwegian–Iceland–Greenland seas, overlain by Upper North Atlantic Deep Water (UNADW ~1600–~2300 m) originating from the Labrador Sea. Lower Deep Water (LDW) containing a significant fraction of water from the South Atlantic covers the deeper BOR, below 4500 m [28,16]. The WBUC extends below 4500 m and is therefore not exclusively composed of NSW [28,29].

We compare our results with published data from ODP Site 1059 also at BOR (126 km from Site 1060, at 2985 m water depth) [30].

3. Methods

3.1. Grain size analysis

McCave et al. [25] suggested that the mean grain size of the 10–63 μm terrigenous fraction would provide a more sensitive indicator of current speed than Ledbetter's [31] 'silt mean size', size range 4–63 μm. The fraction finer than 10 μm should be left out of the calculation of the mean silt size because clay and fine silt are deposited as aggregates and not sorted by primary particle size. The 'sortable silt' mean grain size ($\overline{SS}$), which varies independently of sediment supply in current-sorted and deposited muds, has been used as an established proxy for flow speed in many studies (see review by McCave and Hall [26]).

Prior to analysis, coarse material (>63 μm) was removed by wet sieving. Samples were treated with dilute acetic acid (1 M) to remove calcium carbonate and heated sodium carbonate (2 M) to remove biogenic opal. All samples contained silt concentrations exceeding 5%, giving precisions in $\overline{SS}$ determinations of ±1.5% [32]. Grainsizes were analyzed using a Coulter Counter Multisizer 3, as this produces reliable measurements for smaller (<1 g) samples [32].

3.2. Isotopic and trace element analysis

Vautravers et al. [33] use benthic carbon isotope data ($\delta^{13}C$, based on 4 specimens of *Uvigerina peregrina*), measured using a VG Prism mass spectrometer with analytical precision of ±0.06‰ for $\delta^{13}C$, (and ±0.08‰ for $\delta^{18}O$) at ODP Site 1060. We measured Cd/Ca ratios on *U. peregrina* for a selected period (~46–52 ka), characterized by large scale changes in $\delta^{13}C$ (*U. peregrina*) as well as in flow vigour. Unlike $\delta^{13}C$, Cd/Ca measured on different benthic foraminiferal species

[2] To avoid calling ancient water masses by modern names with a 'Glacial' prefix, which carries unwarranted assumptions about formation processes, we prefer to use simply Northern and Southern Source (NS, SS) designations with the usual Intermediate and Deep Water (IW, DW) and G for glacial modifiers. Use of, e.g., LNADW applies only to the modern situation.

(both infaunal and epibenthic), may not be species-dependent as different species show similar results [34]. For Cd/Ca analysis a minimum of 10 specimens of *U. peregrina*, weighing at least 500 μg, were picked, gently crushed between two glass plates, and cleaned following the method described by Yu et al. [35]. Cd/Ca ratios in *U. peregrina* were measured using the method developed by Yu et al. [35], involving direct measurement of intensity ratios on a quadrupole inductively coupled plasma-mass spectrometer (ICP-MS) using external, matrix-matched standards.

4. Age model

The age model for Site 1060 is initially derived from Vautravers et al. [33], and based on the assumption that

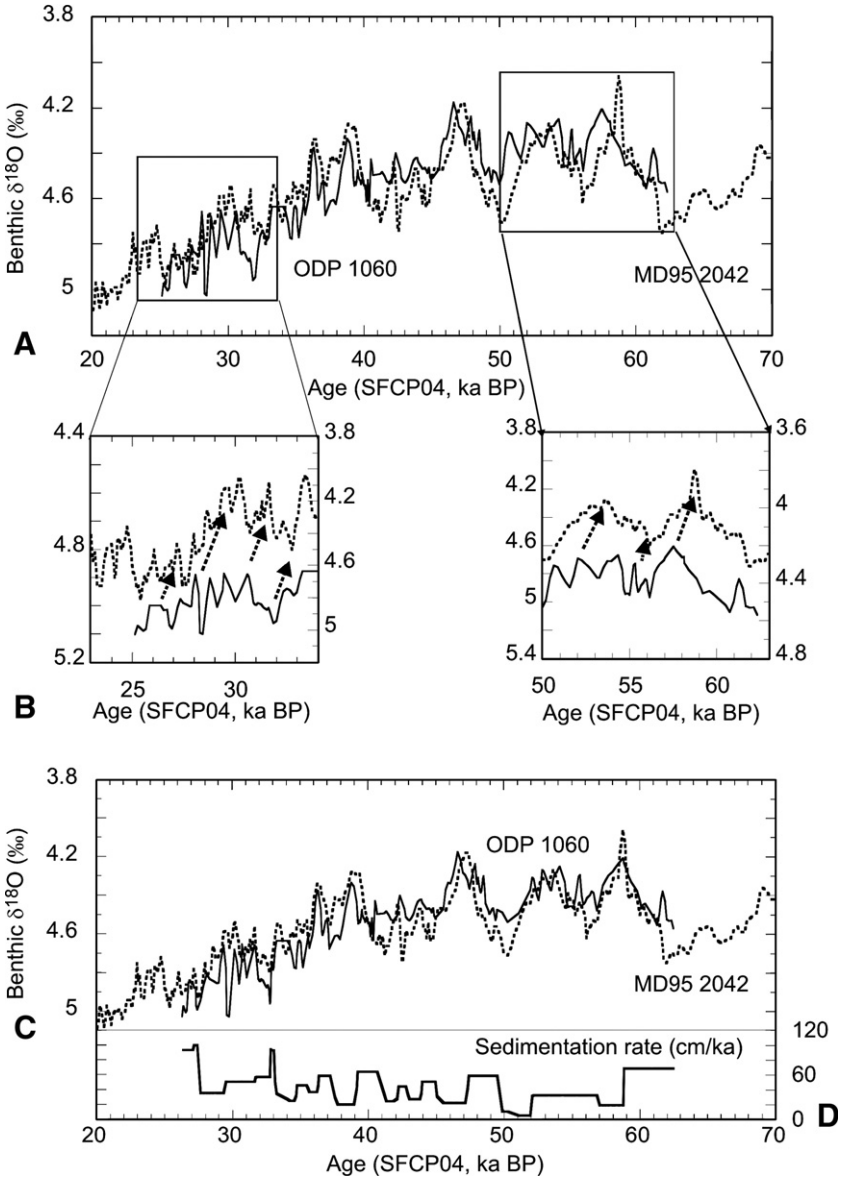

Fig. 2. A—Comparison benthic foraminiferal (*U. peregrina*) δ^{18}O of ODP Site 1060 (solid line, 1-2-1 weighted three point smoothing) with that of MD95-2042 (*Globobulimina affinis, Cibicidoides wuellerstorfi and U. peregrina* from Shackleton et al. [60] (dotted line) against the SFCP04 age scale. The two intervals indicated by boxes show periods where the two records do not match (ODP 1060 lags MD95-2042). B—Correction of the age scale for the two intervals, where the age scale of ODP 1060 has been adjusted to agree with that of MD95-2042. C—Comparison of benthic foraminiferal δ^{18}O of ODP Site 1060 with that of MD95-2042 after the age scale correction of ODP 1060.

sea surface temperatures (SST) at Site 1060, inferred from the percentage warm planktonic foraminiferal species, respond similarly and with no appreciable delay to climate variations as recorded in the GRIP ice core from Greenland. This is supported by the simultaneous shifts off North Venezuela with those at Greenland argued by Hughen et al. [36] on ultra-high resolution records. However the time scale for the ice core used here is not the current glaciological age scale, 'ss09sea' of Johnsen et al. [37] but the newly proposed age scale for the Greenland ice cores (the SFCP04 timescale of Shackleton et al. [38]) because this is better in the lower part of MIS 3 [39]. This age scale assigns ages of 29 and 59 ka to the bases of Greenland interstadials 2 and 17 respectively and interpolates according to the ss09sea glaciological scale. Age control points were tied by correlation of planktonic foraminiferal species abundances ('% warm species') at BOR to variations of the planktonic foraminiferal oxygen isotope record (δ^{18}O) of core MD95-2042 (37°48′ N, 10°10′ W, 3146 m) off Portugal on which the SFCP04 timescale is based. However, there may be problems associated with this approach. The assumption that West Atlantic SST, East Atlantic δ^{18}O and central Greenland temperature varied synchronously may be questioned. In addition, the percentage of warm planktonic foraminiferal species may also be influenced by differential carbonate dissolution of the various planktonic species, for example due to changes in the bottom water masses, or respiration-driven dissolution. At the shallower BOR Site (2985 m), Hagen and Keigwin [30] show that the timings and durations of stadial and interstadial periods between 40 and 60 ka determined by the % of *Globigerinoides ruber* (the "warm" group is mainly made up of *G. ruber* and *G. sacculifer*) diverge from those obtained from δ^{18}O (*G. ruber*), showing that the % warm planktonic foraminiferal species does not correlate exactly with δ^{18}O.

Such potential age-constraint issues can be tested by comparison with an independent age model. The low concentration of planktonic foraminifera prohibits the development of continuous planktonic δ^{18}O, or the acquisition of AMS radiocarbon dates [33]. Therefore we compare benthic foraminiferal δ^{18}O values (*U. peregrina*) from Site 1060 to those (*Globobulimina affinis*, *Cibicidoides wuellerstorfi* and *U. peregrina*) of MD95-2042, and thence to the SFCP04 timescale (Fig. 2). However, this too is open to question as the two sites are in different (western and eastern) basins of the North Atlantic with different supply routes for SSW which presently influences MD95-2042 significantly [40] but ODP 1060 negligibly [28]. Nevertheless, the two benthic δ^{18}O records are very similar and show the same trends, suggesting that deep ocean hydrographic properties (temperature and salinity) at these two similar depths and latitudes in the North Atlantic Ocean were also similar. Between 50 and 60 ka and between 25 and 32 ka, changes in δ^{18}O of Site 1060 appear to lag those at MD95-2042 by 1 to 2×10^3 yr (Fig. 2). This is most unlikely. Even given east/west basin differences, appearance/disappearance of SSW should not differ by more than a few hundred years. We therefore corrected the age model of Site 1060 at these two intervals (50–60 ka and 25–32 ka), by correlating benthic δ^{18}O at Site 1060 to MD95-2042 (Fig. 2). This correction results in rather low sediment accumulation rates between 51 and 53 ka, indicating either a small hiatus or a problem with the ages of MD95-2042.

5. Results

5.1. Flow vigour

The overall shape of the flow speed proxy record shows a complex pattern of variability, with the highest flow speeds (higher $\overline{SS}$ values) tending to occur in warm D/O interstadials, apart from those in MIS 2 (Fig. 3). During the majority of MIS 3 (35–60 ka) bottom flow speed was more vigorous than in the younger part of MIS 3 (<35 ka) and the following MIS 2, where from 35 ka on flow speed was reduced (Fig. 3). The $\overline{SS}$ record also shows the largest variations over the period 35–60 ka, whereas the following period (20–35 ka) displays smaller variations in $\overline{SS}$ (Fig. 3).

Although at first glance there is some similarity between our $\overline{SS}$ record and % warm species and the GRIP δ^{18}O between ~50 and 40 ka, over the record as a whole, similarities are less clear (Fig. 3). Within MIS 3 six intervals are characterized by large reductions in bottom flow speed, centred around 34, 41, 44, 49, 54 and 61 ka, which are here termed 'Slow Events' (SEs) 0, 1, 1a, 2, 3 and 4. There is no clear relationship between flow vigour at Site 1060 and D/O cycles (Figs. 3 and 4). Instead there appears to be a close match between SEs and warming phases of Antarctic Warm Events A1 to A4 (with one new one, A1a and one poorly defined A0) (Fig. 4). All periods of reduced flow vigour correspond to warming phases of Antarctic Warm Events, and in most instances even short intervals of cooling within the broader Antarctic warming phases are coupled with brief intervals of invigoration of flow intensity.

A possible D/O feature is that stadial 12 (after interstadial 12) is associated with a large reduction in flow speed (SE1a), followed by a rapid increase in flow

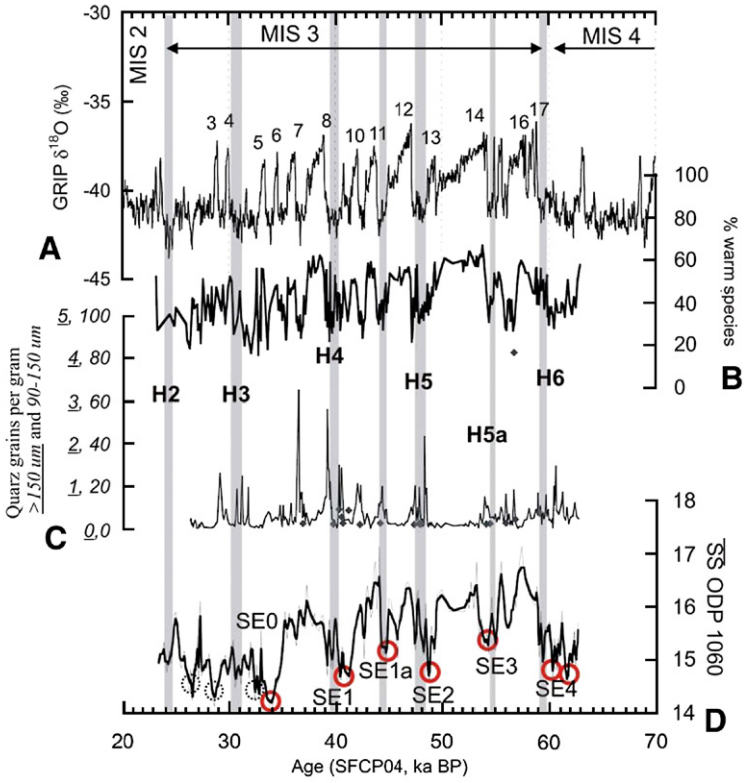

Fig. 3. A — GRIP ice $\delta^{18}O$ [4], B — ODP 1060 planktonic foraminifera % warm species, C — ODP 1060 number of quartz grains per gram in the 90–150 μm (solid line) and>150 μm fraction (grey diamonds), and D — ODP 1060 mean grainsize ($\overline{SS}$) of the sortable silt fraction (10–63 mm). Planktonic foraminiferal %warm species and IRD data are from Vautravers et al. [33]. A 1-2-1 weighted three point smoothing (thin grey line) and 1-2-3-2-1 (thick black line) smoothing were applied to the $\overline{SS}$ data. Several D/O interstadials and Heinrich events (H, grey bars) are indicated, and H5a (S15) was added by Rashid et al. [41]. Also indicated are ′slow events′ of reduced flow vigour SE0 to SE4 (thick lined circles).

speed during interstadial 11. Heinrich events H3, H4 and H5 do not coincide with slow flow but are all preceded by flow speed minima (SE0, SE1, and SE2 respectively). Lastly, Heinrich event H5a/Stadial 15 [41] appears associated with a decrease in flow vigour (SE3), lasting well into the following warm interstadial 14 (Fig. 3).

5.2. Bottom water properties

The $\delta^{13}C$ (*U. peregrina*) record of Site 1060 shows a similar pattern to the GRIP $\delta^{18}O$ record and the Site 1060 % warm species, with generally lower $\delta^{13}C$ values during intervals of cooler surface water [33]. Comparison with $\delta^{13}C$ records (*Cibicidoides* and *U. peregrina*) from ODP 1059 (2985 m) shows very similar trends (Fig. 5). Short-term $\delta^{13}C$ decreases during stadials and Heinrich events are correlated with abrupt increases in wind intensity [42] which may have led to higher nutrient input by mixing, and thus higher productivity and export of organic matter (higher amounts of preserved diatoms were observed during Heinrich 5). We suggest that the short-term $\delta^{13}C$ variability is mainly controlled by export and decomposition of marine organic matter rather than bottom water mass changes as suggested by Vautravers et al. [33].

Both *U. peregrina* records from Site 1059 and 1060 have similar ranges during MIS 3 of ~1.2‰ (note that the records in Fig. 5 are smoothed by a 5 point moving average: the smoothed range is ~0.8‰). However, at Site 1059 $\delta^{13}C$ varies around a mean of −1.0‰, whereas at the deeper Site 1060 $\delta^{13}C$ the mean is −1.25‰. This ~0.25‰ difference is very similar to the difference found during the LGM using epibenthic species which may record the water mass properties more faithfully [43]. Although there is a pore water influence on $\delta^{13}C$ records of infaunal *U. peregrina* [44–46], because the two sites show such similar variations in *U. peregrina* $\delta^{13}C$ we attribute differences in the *mean* $\delta^{13}C$ to nutrient related water mass properties.

Cd/Ca ratios measured on *U. peregrina* for a selected period (~47–53 ka) show lower values (0.06–

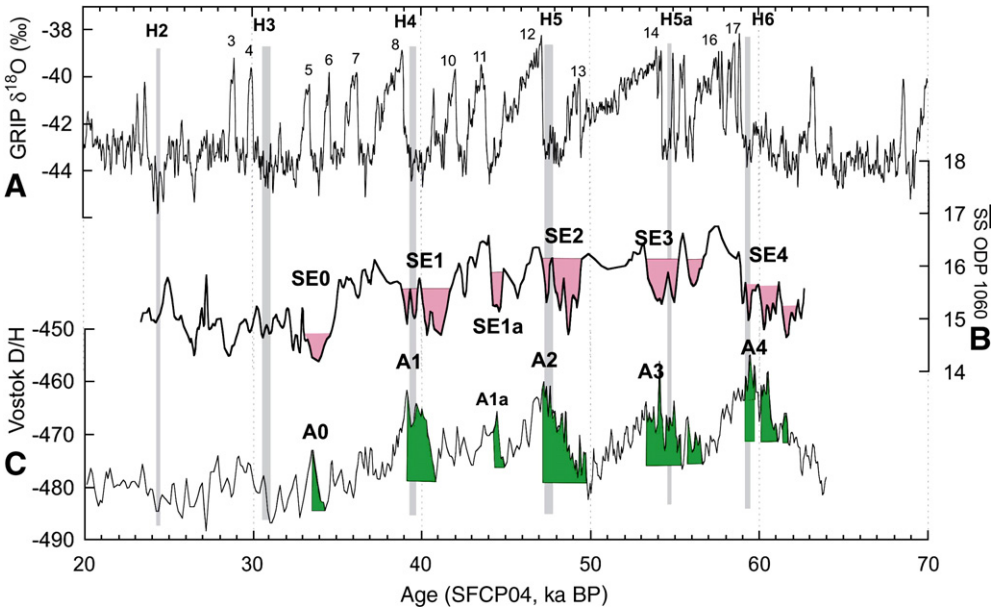

Fig. 4. A — GRIP ice $\delta^{18}O$ [4] with most D/O interstadials and Heinrich events H2–H6 (grey bars), B — ODP 1060 $\overline{SS}$, and C — Antarctic Vostok D/H ratio [69], on the SFCP04 age scale. Also indicated are Antarctic warming events A0 to A4 (note A0 is a newly defined warm event), and 'slow events' of reduced flow vigour SE0 to SE4. To compare the timing relationship of SEs with Antarctic warming, SE0 to SE4 are highlighted with a pink background filling, whereas periods of Antarctic warming associated with A0 to A4 are highlighted by a green background filling.

0.07 mmol/mol), indicating the presence of low-nutrient bottom or pore water, at the site over the younger part of interstadial 14 and the start of interstadial 12, whereas higher values occur during the later part of interstadial 14 until the start of interstadial 12 (Fig. 5). These results suggest that bottom or pore waters were more nutrient-rich at Site 1060 between interstadials 14 and 12 (47–50 ka) across H5, whereas $\delta^{13}C$ at Sites 1060 and 1059 suggest more nutrient-rich bottom waters only during H5. However, the interval 47–50 ka is also a time of higher wind stress and potentially higher productivity [42]. Thus it is possible that the increase in Cd/Ca during this period also resulted from a stronger source of decaying organic matter [47].

Short term benthic foraminiferal $\delta^{13}C$ and potentially Cd/Ca variations at Site 1060 (and 1059) probably do not reliably reflect bottom water mass changes, but are instead largely affected by variations in supply and decomposition of organic material mainly derived from surface ocean productivity. For this reason the benthic foraminiferal $\delta^{13}C$ properties resemble the phasing of events in Greenland. However during interstadial 14 it is possible that the *Cibicides* $\delta^{13}C$ record does reflect bottom water mass changes – mixing in of more ^{13}C-depleted SSW – as there are no large increases in inferred wind intensity and thus productivity between 52 and 55 ka [42].

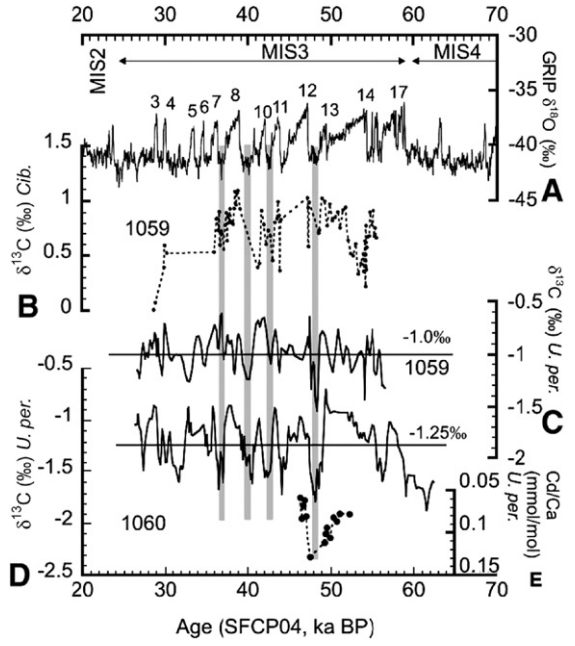

Fig. 5. A — GRIP ice $\delta^{18}O$ [4] with most D/O interstadials numbered; B — epibenthic $\delta^{13}C$ ODP 1059 (*Cibicidoides*); and C — infaunal $\delta^{13}C$ ODP 1059 (*U. peregrina*) [30]; D — infaunal $\delta^{13}C$ ODP 1060 (*U. peregrina*) [33]; and E — Cd/Ca measured on infaunal *U. peregrina* (ODP 1060), all on the SFCP04 age scale. A, C and D were all smoothed using a 1-2-1 weighted three point smoothing.

6. Discussion

It has been suggested that millennial scale climate variations may be linked to changes in the mode and strength of thermohaline circulation [3,48,49]. In the northern hemisphere D/O stadial intervals within MIS 3 are characterized by significant coolings and are thought to be associated with suppression of GNSDW formation leaving GNSIW as the major subsurface but not 'deep' water of northern origin, and even cessation of convective water mass transformation during the extreme stadial Heinrich events [3,12]. During these Heinrich events fresh water, released by melting of icebergs, is thought to decrease the sea surface salinity (SSS) and thus density in the North Atlantic resulting in a reduction in deep water formation by convection [49–52]. Modelling experiments show that increased fluxes of freshwater to sites of North Atlantic Deep Water formation cause a decrease in deep water formation, resulting in reduced meridional heat transport with cooling in the northern North Atlantic and warming in the southern South Atlantic [53,54].

Carbon isotope values of *U. peregrina* for Site 1060 and the shallower site 1059 show an overall $\delta^{13}C$ difference of ~0.25‰ between the two sites, close to that reported by Curry and Oppo [43] for epibenthic species at the LGM. We interpret this as the baseline $\delta^{13}C$ being set by the water mass, but with carbon input variations affecting signal magnitude at the two sites simultaneously by about the same amount. For the LGM, Curry and Oppo [43] propose SSW to occupy water depths >2000 m with South Atlantic values below 4000 m, indicating strong vertical mixing in a transition zone between the Northern and Southern source end members. This is confirmed by the fact that the absolute values of $\delta^{13}C$ for *C. wuellerstorfi* at Sites 1059 and 1060 are mainly above +0.5‰ whereas the same species in the glacial South Atlantic SSW source region in MIS 3 has values always below zero and down to −0.8‰ [30,33,55]. The values at BOR thus represent a significant degree of mixing of this end-member with shallow nutrient-depleted water of $\delta^{13}C > 1.2$‰ [43].

Reconstructed bottom current intensity at ~3500 m generally does not correspond with Greenland millennial scale climate variability but closely matches periods of Antarctic warming, A1–A4. These results do not show what would be expected if northern convective activity controlled deep flow. The possible connections between coincidence of large-scale reductions in flow speed with Antarctic warming are either reduced volume flux of SSW due to lower production rate or reduction in SSW density (warmer and/or less salty) leading to reduced geostrophic flow (or both). It is important to note that we are dealing with transient, unsteady-state behaviour. The warming limb of Antarctic events A1–A4 last no more than 2 overturn times of the modern ocean (less than ~3000 yr). Thus the slow down in speed corresponds to the period of decreasing benthic $\delta^{18}O$ and ends at its minimum (Fig. 2).

Antarctic warming would involve warmer SST and probable decreased sea-ice export from around Antarctica, which, in the model of Keeling and Stephens [56] would reduce the salinity of sinking Southern Ocean waters. This argument is corroborated by Kaiser et al. [57] who argue that enhanced westerly wind transport around Antarctic during Antarctic coolings caused increased northerly Ekman drift of sea-ice, whereas during warmings the Westerlies were confined to more polar latitudes causing decreased sea-ice export.

Although the record of Wolff et al. [58] suggests no significant changes in sea-ice production over the younger part of MIS 3, Wolff et al. [59] show clear antiphase changes in Na concentration and δD at EPICA Dome C. Thus there may have been decreased sea-ice production during Antarctic warmings and reduction in deep water salinity associated with brine rejection by sea-ice. It is therefore expected that SSW density was reduced during warming phases of Antarctic Warm Events by both lower salinity and increased temperature. Shackleton et al. [60] attribute deep benthic $\delta^{18}O$ changes at the Iberian margin to a combination of ice volume and temperature changes. Sea-level variations of up to ~35 m proposed for MIS 3 [61,62] would account for 0.3‰ of the 0.5‰ amplitude of variability demonstrated by Shackleton et al. [60], leaving 0.2‰ to be attributed to temperature changes. With 1‰ ~4 °C, that would be ~0.8 °C, similar to estimates from Adkins et al. [63], giving a reduction in density (σ(Stp)) at 0 to 0.8 °C of 0.15 kg m^{-3}. Deep water temperature changes with the warming and cooling phases of the Antarctic Warm Events would then result in reduction of bottom water density during warming, and increase during cooling. This would have a significant effect on the geostrophic flow of the Glacial WBUC. For example with the flow speed of the lower layer in a two layer system given by $U = ig\Delta\rho/\rho f$ (i is slope of the interface between water masses of density difference $\Delta\rho$, (lower one of density ρ), and Coriolis parameter f), the change in flow speed caused by reducing the density contrast $\Delta\rho$ by $\delta\Delta\rho$ (0.15 kg m^{-3} in this case) would be $U\delta\Delta\rho/\Delta\rho$, holding i constant. As typical density differences between modern Labrador Sea Water and Lower Deep Water are less than 1 kg m^{-3}, the speed reduction is expected to be more than 20%.

These results show that the flow variability of the lower limb of the WBUC was not connected to sharp North Atlantic changes in temperature. This means that it is unlikely that the D/O cycles were associated with a mode of MOC variation involving whole-ocean overturn, but more likely with perturbations of the shallow Glacial Gulf Stream-GNSIW cell as depicted in Rahmstorf's [3] well known cartoon.

Because the locus of filaments of locally faster and slower flow is dependant on density structure, the whole picture cannot be deduced from one point. In order to fully determine whether the GWBUC as a whole was significantly reduced in strength or whether the fastest filament of the flow migrated with the Northern Hemisphere millennial climate fluctuations, a depth transect of shallower core sites along an appropriate transect avoiding shelf/slope influences will need to be studied. Such information is not only crucial for MIS 3, but also for the LGM. Models predicting ocean circulation during the LGM [64–66] are contradictory and presently poorly validated by consistent multi-proxy experimental data. As a result, the state of meridional transport intensity is poorly constrained, crucial though it is to understanding climate change.

7. Conclusions

A direct flow speed proxy (mean grain size of the sortable silt) suggests a complex pattern of variability of the flow vigour of the North Atlantic's deep western boundary current during MIS 3 at 3481 m water depth (ODP Site 1060, Blake Outer Ridge,). Overall flow speed was more vigorous between 35 and 60 kyr, showing large-scale variability, while the remainder of MIS 3 (<35 ka) and MIS 2 (LGM) are characterized by slower flows, and only small variations. Within MIS 3, 'slow events' of reduced flow speed are seen centred around 34, 41, 44, 49, 54 and 61 ka, (SE0 to SE4). All SEs can be correlated to warming phases of Antarctic Warm Events but appear uncorrelated to Greenland climate variability. Antarctic climate therefore exerted a stronger influence on deep flow vigour in the North Atlantic during MIS 3 than Northern Hemisphere climate. The connection between SEs and major Antarctic warmings suggests that either the volume flux of SSW being produced was reduced and/or the density was reduced, giving a smaller density contrast and weaker geostrophic flow.

These results do not show the expected pattern if northern convective activity controlled deep flow. Instead it seems that D/O cycles were associated with a mode of MOC variation involving perturbations of only the shallow Glacial Gulf Stream-GNSIW cell. This, being much shallower, would respond more rapidly to northern fresh water forcing than a circulation involving the whole 5000 m of the Atlantic. The results also offer no support to the suggestion that there were massive convective perturbations to the deep ocean flow following Heinrich Events [63]. The possibility that the flow speed reductions were due to reduced wind-driven sea-ice export (and consequential reduced brine input to bottom water) implies that cold phase winds around Antarctica were stronger, and warm phase winds weaker, counter to some recent model-based suggestions [67].

Hydrographic conditions at Sites 1060 (3481 m) and 1059 (2985 m) during MIS 3 may have been similar to those of the LGM, because there is a consistent carbon isotope gradient of ~ -0.25‰ between these Sites. This suggests that the WBUC at 3500 m was in the mixing zone between Northern and Southern Source Waters during MIS 3. Short-term variations in benthic foraminiferal $\delta^{13}C$, that appear synchronous with Greenland climate variability, are attributed to changes in the input fluxes of marine organic material and decomposition in bottom sediments, with increased input during stadials and Heinrich events attributed to increased wind intensity/mixing and surface productivity.

In order to fully address whether the GNSDW/GNSIW component of the GWBUC was significantly reduced in strength and/or migrated in association with the Northern Hemisphere millennial scale climate fluctuations, a depth transect of shallower core sites along BOR will need to be studied. The data shown in this paper are available at: http://www.ncdc.noaa.gov/paleo/paleocean.html.

Acknowledgements

We are very grateful to Mike Cooke, Gillian Foreman, Mervyn Greaves, Jo Hellawell, Jake Lack, Luke Skinner and Jimin Yu, for assistance with sample preparation and analysis and advice and discussion. Sveinung Hagen and Lloyd Keigwin provided access to data from ODP Site 1059. This research used samples and/or data provided by the Ocean Drilling Program (ODP). ODP is sponsored by the U.S. National Science Foundation and participating countries (Natural Environment Research Council in UK) under management of Joint Oceanographic Institutions (JOI), Inc. This work was supported by the Isaac Newton Trust, University of Cambridge. Funding for $\delta^{18}O$ measurements was provided by EC Grant EVK2-2000-0089 (MV). We are grateful to the reviewers for helpful comments, which improved the paper.

Appendix A. Supplementary data

Supplementary data associated with this article can be found in the online version, at doi:10.1016/j.epsl.2007.03.003.

References

[1] W. Dansgaard, S.J. Johnsen, H.B. Clausen, D. Dahl-Jensen, N.S. Gundestrup, C.U. Hammer, C.S. Hvidberg, J.P. Steffensen, A.E. Sveinbjornsdottir, J. Jouzel, G. Bond, Evidence for general instability of past climate from a 250 kyr ice core, Nature 364 (1993) 218–219.

[2] P.M. Grootes, M. Stuiver, J.W.C. White, S. Johnsen, J. Jouzel, Comparison of oxygen isotope records from the GISP2 and GRIP Greenland ice cores, Nature 366 (1993) 552–554.

[3] S. Rahmstorf, Ocean circulation and climate during the past 120,000 years, Nature 419 (2002) 207–214.

[4] S.J. Johnsen, H.B. Clausen, W. Dansgaard, K. Fuhrer, N. Gundestrup, C.U. Hammer, P. Iversen, J. Jouzel, B. Stauffer, J.P. Steffensen, Irregular glacial interstadials recorded in a new Greenland ice core, Nature 359 (1992) 311–313.

[5] P.A. Mayewski, L.D. Meeker, M.S. Twickler, S. Whitlow, Q. Yang, W.B. Lyons, M. Prentice, Major features and forcing of high-latitude northern hemisphere atmospheric circulation using a 110,000-year-long glaciochemical series, J. Geophys. Res. 102 (1997) 26,345–26,366.

[6] I. Cacho, J.O. Grimalt, C. Pelejero, M. Canals, F.J. Sierro, J.A. Flores, N. Shackleton, Dansgaard-Oeschger and Heinrich event imprints in Alboran Sea paleotemperatures, Paleoceanography 14 (1999) 698–705.

[7] J.P. Sachs, S.J. Lehman, Subtropical North Atlantic temperatures 60,000 to 30,000 years ago, Science 286 (1999) 756–759.

[8] S. van Kreveld, M. Sarnthein, H. Erlenkeuser, P. Grootes, S. Jung, M.J. Nadeau, U. Pfaumann, A. Voelker, Potential links between surging ice sheets, circulation changes, and the Dansgaard-Oeschger cycles in the Irminger Sea, 60–18 kyr, Paleoceanography 15 (2000) 425–442.

[9] H. Heinrich, Origin and causes of cyclic ice rafting in the northeast Atlantic during the past 130,000 years, Quat. Res. 29 (1988) 142–152.

[10] G. Bond, W.S. Broecker, S. Johnsen, J. McManus, L. Labeyrie, J. Jouzel, G. Bonani, Correlations between climate records from North Atlantic sediments and Greenland ice, Nature 365 (1993) 143–147.

[11] W.S. Broecker, Massive iceberg discharges as triggers for global climate change, Nature 372 (1994) 421–424.

[12] M. Sarnthein, K. Winn, S.J.A. Jung, J.-C. Duplessy, L. Labeyrie, H. Erlenkeuser, G. Ganssen, Changes in east Atlantic deepwater circulation over the last 30,000 years: eight time slice reconstructions, Paleoceanography 9 (1994) 209–267.

[13] P. LeGrand, C. Wunsch, Constraints from paleotracer data on the North-Atlantic circulation during the last glacial maximum, Paleoceanography 10 (1995) 1011–1045.

[14] T.C. Johnson, E.L. Lynch, W.J. Showers, N.C. Palczuk, Pleistocene fluctuations in the western boundary undercurrent on the Blake Outer Ridge, Paleoceanography 3 (1988) 191–207.

[15] E.F. Yu, R. Francois, M.P. Bacon, Similar rates of modern and last-glacial ocean thermohaline circulation inferred from radiochemical data. Nature 379 (1996) 689–694.

[16] W.S. Schmitz, M.S. McCartney, On the North Atlantic circulation, Rev. Geophys. 31 (1993) 29–49.

[17] M.T. Ledbetter, W.L. Balsam, Paleoceanography of the deep Western Boundary Undercurrent on the North Atlantic continental margin for the past 25,000 yr, Geology 13 (1985) 181–184.

[18] B.J. Haskell, T.C. Johnson, W.J. Showers, Fluctuations in the deep western North Atlantic circulation on the Blake Outer Ridge during the last deglaciation, Paleoceanography 6 (1991) 21–31.

[19] G.G. Bianchi, M. Vautravers, N.J. Shackleton, Deep flow variability under apparently stable North Atlantic Deep Water production during the last interglacial of the subtropical NW Atlantic, Paleoceanography 16 (2001) 306–316.

[20] S.O. Franz, R. Tiedemann, Depositional changes along the Blake–Bahama Outer Ridge deep water transect during marine isotope stages 8 to 10 — links to the Deep Western Boundary Current, Mar. Geol. 189 (2002) 107–122.

[21] M. Yokokawa, S.O. Franz, Changes in grain size and magnetic fabric at Blake–Bahama Outer Ridge during the late Pleistocene (Marine Isotope Stages 8–10), Mar. Geol. 189 (2002) 123–144.

[22] D.W. Oppo, S.J. Lehman, Mid-depth circulation of the subpolar North Atlantic during the last glacial maximum, Science 259 (1993) 1148–1152.

[23] F.R. Stahr, T.B. Sanford, Transport and bottom layer observarions of the North Atlantic deep western boundary current at the Blake Outer Ridge, Deep-Sea Res. II 46 (1999) 205–243.

[24] W.J. Jenkins, P.B. Rhines, Tritium in the deep North Atlantic Ocean, Nature 286 (1980) 877–880.

[25] I.N. McCave, B. Manighetti, S.G. Robinson, Sortable silt and fine sediment size/composition slicing: parameters for palaeocurrent speed and palaeoceanography, Paleoceanography 10 (1995) 593–610.

[26] I.N. McCave, I.R. Hall, Size sorting in marine muds: processes, pitfalls and prospects for paleoflow-speed proxies, Geochem. Geophys. Geosyst. 7 (2006) doi:10.1029/2006GC001284.

[27] G.M. Bryan, Hydrodynamic model of Blake Outer Ridge, J. Geophys. Res. 75 (1970) 4530–4538.

[28] A.F. Amos, A.L. Gordon, E.D. Schneider, Water masses and circulation patterns in the region of Blake–Bahama Outer Ridge, Deep-Sea Res. 18 (1971) 145–165.

[29] G.L. Weatherly, E.A. Kelley, Two views of the cold filament, J. Phys. Oceanogr. 15 (1984) 68–81.

[30] S. Hagen, L.D. Keigwin, Sea-surface temperature variability and deep water reorganisation in the substropical North Atlantic during Isotope Stage 2–4, Mar. Geol. 189 (2002) 145–162.

[31] M.T. Ledbetter, Fluctuations of Antarctic Bottom Water velocity in the Vema Channel during the last 160,000 years, Mar. Geol. 33 (1–2) (1979) 71–89.

[32] G.G. Bianchi, I.R. Hall, I.N. McCave, L. Joseph, Measuring the sortable silt current speed proxy using the Sedigraph 5100 and Coulter Multisizer IIe: precision and accuracy, Sedimentology 46 (1999) 1001–1014.

[33] M.J. Vautravers, N.J. Shackleton, C. Lopez-Martinez, J.O. Grimalt, Gulf Stream variability during marine isotope stage 3, Paleoceanography 19 (2004) doi:10.1029/2003PA000966.

[34] E. Boyle, Cadmium and δ^{13}C paleochemical ocean distributions during the stage 2 glacial maximum, Annu. Rev. Earth Planet. Sci. 20 (1992) 245–287.

[35] J. Yu, J. Day, M. Greaves, H. Elderfield, Determination of multiple element/calcium ratios in foraminiferal calcite by quadrupole ICP-MS, Geochem. Geophys. Geosyst. 6 (2005) doi:10.1029/2005GC000964.

[36] K. Hughen, S. Lehman, J. Southon, J. Overpeck, O. Marchal, C. Herring, J. Turnbull, ^{14}C activity and global carbon cycle changes over the past 50,000 years, Science 303 (2004) 202–207.
[37] S.J. Johnsen, D. Dahl-Jensen, N. Gundestrup, J.P. Steffensen, H. B. Clausen, H. Miller, V. Masson-Delmotte, A.E. Sveinbjornsdottir, J. White, Oxygen isotope and palaeotemperature records from six Greenland ice-core stations: Camp Century, Dye-3, GRIP, GISP2 Renland and north GRIP, J. Quat. Sci. 16 (2001) 299–307.
[38] N.J. Shackleton, R.G. Fairbanks, T.-C. Chiu, F. Parrenin, Absolute calibration of the Greenland time scale: implications for Antarctic time scales and for $\Delta^{14}C$, Quat. Sci. Rev. 23 (2004) 1513–1522.
[39] C. Spotl, A. Mangini, D.A. Richards, Chronology and paleoenvironment of Marine Isotope Stage 3 from two high-elevation speleothems, Austrian Alps, Quat. Sci. Rev. 25 (2006) 1127–1136.
[40] H.M. Van Aken, The hydrography of the mid-latitude northeast Atlantic Ocean. I: the deep water masses, Deep-Sea Res. I 47 (2000) 757–788.
[41] H. Rashid, R. Hesse, D.J.W. Piper, Evidence for an additional Heinrich event between H5 and H6 in the Labrador Sea, Paleoceanography 18 (2003) doi:10.1029/2003PA000913.
[42] C. López-Martínez, J.O. Grimalt, J. Gruetzner, B. Hoogakker, M.J. Vautravers, I.N. McCave, Abrupt wind regime changes in the north Atlantic Ocean during the past 30000–60000 years, Paleoceanography 21 (2006) PA4215 doi:10.1029/2006PA001275.
[43] W.B. Curry, D.W. Oppo, Glacial water mass geometry and the distribution of $\delta^{13}C$ of CO_2 in the western Atlantic Ocean, Paleoceanography 20 (2005) doi:10.1029/2004PA001021.
[44] R. Zahn, K. Winn, M. Sarnthein, Benthonic foraminiferal $\delta^{13}C$ and accumulation rates of organic carbon: *Uvigerina peregrina* group and *Cibicidoides wuellerstorfi*, Paleoceanography 1 (1986) 27–42.
[45] R. Zahn, A. Rushdi, N.G. Pisias, B.D. Bornhold, B. Blaise, R. Karlin, Carbonate deposition and benthonic $\delta^{13}C$ in the subarctic Pacific: implications for changes of the oceanic carbonate system during the past 750,000 years, Earth Planet. Sci. Lett. 103 (1991) 116–132.
[46] A. Mackensen, H.-W. Hubberten, T. Bickert, G. Fischer, D.K. Fütterer, The $\delta^{13}C$ in benthonic foraminiferal tests of *Fontbotia wuellerstorfi* (Schwager) relative to the $\delta^{13}C$ of dissolved inorganic carbon in southern ocean deep water: implications for glacial ocean circulation models, Paleoceanography 8 (1993) 587–610.
[47] K. Tachikawa, H. Elderfield, Chemistry of benthic foraminiferal shells for recording ocean environments: Cd/Ca, $\delta^{13}C$ and Mg/Ca, in: Shiyomi, et al., (Eds.), Global Environmental Change in the Ocean and on Land, 2004, pp. 249–263.
[48] E.A. Boyle, Is ocean thermohaline circulation linked to abrupt stadial/interstadial transitions? Quat. Sci. Rev. 19 (2000) 255–272.
[49] W.S. Broecker, Abrupt climate change: causal constraints provided by the paleoclimate record, Earth-Sci. Rev. 51 (2000) 137–154.
[50] M.A. Maslin, N.J. Shackleton, U. Pfaumann, Surface-water temperature, salinity and density changes in the Northeast Atlantic during the last 45,000 years — Heinrich events, deep-water formation, and climatic rebounds, Paleoceanography 10 (1995) 527–544.
[51] L. Vidal, L. Labeyrie, E. Cortijo, M. Arnold, J.C. Duplessy, E. Michel, S. Becque, T.C.E. van Weering, Evidence for changes in the North Atlantic Deep water inked to meltwater surges during Heinrich events, Earth Planet. Sci. Lett. 146 (1997) 13–27.
[52] R. Zahn, J. Schonfeld, H.-R. Kudrass, M.-H. Park, H. Erlenkeuser, P. Grootes, Thermohaline instability in the North Atlantic during meltwater events: stable isotope and ice-rafted detritus records form core SO75-26KL, Portuguese margin, Paleoceanography 12 (1997) 696–710.
[53] A. Ganopolski, S. Rahmstorf, Rapid changes of glacial climate simulated in a coupled climate model, Nature 409 (2001) 153–158.
[54] R. Knutti, J. Fluckiger, T.F. Stocker, A. Timmermann, Strong hemisphere coupling of glacial climate through freshwater discharge and ocean circulation, Nature 430 (2004) 851–856.
[55] U.S. Ninnemann, C.D. Charles, Changes in the mode of Southern Ocean circulation over the last glacial cycle revealed by foraminiferal stable isotopic variability, Earth Planet. Sci. Lett. 201 (2002) 383–396.
[56] R.F. Keeling, B.B. Stephens, Antarctic sea ice and the control of Pleistocene climate instability, Paleoceanography 16 (2001) 112–131.
[57] J. Kaiser, F. Lamy, D. Hebbeln, A 70-kyr sea surface temperature record off southern Chile (Ocean Drilling Program Site 1233), Paleoceanography 20 (2005) doi:10.1029/2005PA001146.
[58] E.W. Wolff, E.M. Rankin, R. Röthlisberger, An ice core indicator of Antarctic sea ice production? Geophys. Res. Lett. 30 (2003) doi:10.1029/2003GL018454.
[59] E.W. Wolff, et al., Southern Ocean sea-ice extent, productivity and iron flux over the past eight glacial cycles, Nature 440 (2006) 491–496.
[60] N.J. Shackleton, M.A. Hall, E. Vincent, Phase relationships between millennial-scale events 64,000–24,000 years ago, Paleoceanography 15 (2000) 565–569.
[61] J. Chappell, Sea level changes forced ice breakouts in the Last Glacial cycle: new results from coral terraces, Quat. Sci. Rev. 21 (2002) 1229–1240.
[62] M. Siddall, E.J. Rohling, A. Almogi-Labin, C. Hemleben, D. Meischner, I. Schmeltzer, D.A. Smeed, Sea-level fluctuations during the last glacial cycle, Nature 423 (2003) 853–858.
[63] J.F. Adkins, A.P. Ingersoll, C. Pasquero, Rapid climate change and conditional instability of the glacial deep ocean from the thermobaric effect and geothermal heating, Quat. Sci. Rev. 24 (2005) 581–594.
[64] C.D. Hewitt, A.J. Broccoli, J.F.B. Mitchell, R.J. Stouffer, A coupled model study of the last glacial maximum: was part of the North Atlantic relatively warm? Geophys. Res. Lett. 288 (2001) 1571–1574.
[65] S.J. Kim, G.M. Flato, G.J. Boer, A coupled climate model simulation of the Last Glacial Maximum, Part 2: approach to equilibrium, Clim. Dyn. 20 (2003) 635–661.
[66] S.-I. Shin, Z. Liu, B. Otto-Bliesner, E. Brady, J. Kutzbach, S. Harrison, A simulation of the Last Glacial Maximum climate using the NCAR-CCSM, Clim. Dyn. 20 (2003) 1513–1522.
[67] J.R. Toggweiler, J.L. Russell, S.R. Carson, Midlatitude westerlies, atmospheric CO2, and climate change during the ice ages, Paleoceanography 21 (2006) doi:10.1029/2005PA001154.
[68] I.N. McCave, B.E. Tucholke, Deep current-controlled sedimentation in the western North Atlantic, in: P.R. Vogt, B.E. Tucholke (Eds.), The Geology of North America, Volume M, Geol. Soc. America, Boulder, 1986, pp. 451–468.
[69] J. Jouzel, C. Lorius, J.R. Petit, C. Genthon, N.I. Barkov, V.M. Kotlyakov, V.M. Petrov, Vostok ice core: a continuous isotope temperature record over the last climatic cycle (160,000 years), Nature 329 (1987) 443–445.